NANO LETTERS

2004
Vol. 4, No. 2
313−316

Patterning Nanoscale Structures by Surface Chemistry

Wei Lu* and Dongchoul Kim

Department of Mechanical Engineering, University of Michigan, Ann Arbor, Michigan 48109

Received November 24, 2003; Revised Manuscript Received December 17, 2003

ABSTRACT

This letter reports on a simulation of the nanoscale self-assembly process of a two-phase monolayer on an elastic substrate. Two competing actions determine the phase sizes and their spatial ordering. The phase boundary energy tends to coarsen the phases, while the concentration-dependent surface stress tends to refine the phases. A continuum phase field model is developed, which combines spinodal decomposition, surface stress and surface chemistry. The simulation shows that the self-assembly process can be guided by tuning the surface chemistry of a substrate. An epilayer may evolve into various nanoscale patterns in such a way.

Experiments have shown that a two-phase monolayer on an elastic substrate may self-assemble into nanoscale patterns.[1−4] For instance, a submonolayer of oxygen on a Cu (110) surface can form stable periodic stripes of alternating oxygen overlayer and bare copper.[1] The stripes had a width of about 10 nm and run in the ⟨001⟩ direction. Plass et al. found that a monolayer of Cu and Pb on a Cu (111) surface could form ordered patterns of dots or stripes, depending on the percentage of Pb atoms in the epilayer.[2] These nanoscale self-assembly behaviors are intriguing since they are lacking in a bulk system. If a bulk two-phase alloy is annealed, phases will coarsen to reduce the total area of phase boundary. Time permitting, coarsening will continue until only one large particle is left in a matrix. For a two-phase epilayer, surface stress provides a refining action.[5,6] Surface stress can be roughly viewed as the residual stress in an epilayer multiplied by the layer thickness. It has a unit of force per length and can be measured experimentally.[7−9] For a nonuniform epilayer, the surface stress is also nonuniform, inducing a fringe elastic field in the substrate. When the phase size is reduced, the fringe field depth is reduced, and so is the elastic energy. It is this reduction in the elastic energy that drives phase refining. The two competing actions, coarsening due to phase boundaries and refining due to surface stress, select an equilibrium phase size. Furthermore, a superlattice of dots or stripes may minimize the total free energy, so that the competing actions also drive the self-assembly into the superlattices.[10]

Surface chemistry may be utilized to guide the self-assembly process. To illustrate the idea, consider a two-phase epilayer composed of atomic species A and B. During annealing, the atoms diffuse on the substrate to reduce the free energy. When the substrate surface is homogeneous, the competition of phase boundary and surface stress determines the patterns. However, the locations of self-assembled features cannot be predetermined due to the translational symmetry. Now imagine an inhomogeneous substrate surface and two regions with different affinity to A- and B-atoms. The two regions may both favor the attachment of A- (or B-) atom, or A- and B-atom, respectively. As a result, they either compete to attract the same atom or exchange A- and B-atom. Both actions will change the local average concentration, and thus influence the pattern type. In addition, inhomogeneous surface chemistry may anchor self-assembled features at specific locations. In practice, surface chemistry patterns can be created in several ways. For instance, one may pattern different materials at different locations on a substrate with lithography method. The material pattern then defines a surface chemistry pattern.

In this letter, we report on a simulation of self-assembled two-phase monolayers and the effect of surface chemistry. We have recently proposed a continuous phase field model.[6,11−15] Unlike Vanderbilt and co-workers,[5,10] we do not preassume the pattern types. Our model is a dynamic model and the material system can generate whatever patterns it favors. A sharply defined phase boundary adopted by Vanderbilt and co-workers is unsuitable for such a purpose. A phase boundary in our model is represented by a concentration gradient, an approach analogous to the work of Cahn and Hilliard on spinodal decomposition.[16] In previous works, we have addressed the effect of initial condition, elastic anisotropy and the numerical technique.[12−15] This letter focuses on the effect of surface chemistry. In particular, we will demonstrate how surface chemistry may

* Corresponding author. E-mail: weilu@umich.edu.

10.1021/nl035072d CCC: $27.50
Published on Web 01/07/2004

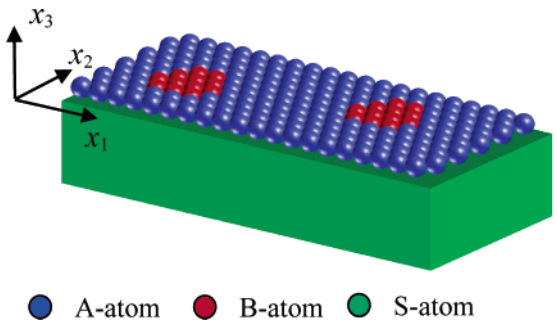

Figure 1. Schematic of self-organized nanoscale patterns on a substrate surface. The substrate occupies the half space $x_3 < 0$ and is bounded by the x_1-x_2 plane.

be used to guide a self-assembly process to make diverse nanoscale patterns.

We first briefly outline the model. Consider an epilayer composed of two atomic species A and B on a substrate of atomic species S, as shown in Figure 1. Both species A and B can be different from S. Alternatively, only one atomic species of the epilayer is different from that of the substrate. The epilayer is treated as an infinitely large surface and the substrate as a semi-infinite elastic body. The substrate occupies the half space $x_3 < 0$ and is bounded by the x_1-x_2 plane. We will simulate the annealing process, where the deposition process has stopped but atoms are allowed to diffuse within the epilayer. The diffusion is driven by free energy reduction. The energy of the system comprises the surface energy in the epilayer and the elastic energy in the substrate. In this paper we assume the substrate is elastically isotropic. The elastic energy per unit volume in the bulk is a quadratic function of strain with Young's modulus E and Possion's ratio ν as material constants. The surface energy per unit area, Γ, takes an unusual form in the model. Define concentration C by the fraction of atomic sites on the substrate surface occupied by species B. Regard the concentration as a spatially continuous and time-dependent function, $C(x_1,x_2,t)$. Generally speaking, when the substrate surface is homogeneous, Γ is a function of the concentration, C, the concentration gradient, $\partial C/\partial x_\alpha$, and the strain in the epilayer, $\epsilon_{\alpha\beta}$ (a Greek subscript runs from 1 to 2). However, when the substrate surface is inhomogeneous, Γ also depends on the local surface chemistry. To consider this effect, we may assume that Γ explicitly depends on the coordinates x_α. Expanding the function $\Gamma(x_\alpha;C,\partial C/\partial x_\alpha,\epsilon_{\alpha\beta})$ in the leading order terms of the concentration gradient $\partial C/\partial x_\alpha$ and the strain $\epsilon_{\alpha\beta}$, we have

$$\Gamma = g + h\left(\left(\frac{\partial C}{\partial x_1}\right)^2 + \left(\frac{\partial C}{\partial x_2}\right)^2\right) + f(\epsilon_{11} + \epsilon_{22}) \qquad (1)$$

where g, h, and f are all functions of the concentration C and coordinates. We have assumed that h and f are isotropic in the plane of the surface. The leading-order term in the concentration gradient is quadratic because, by symmetry, the term linear in the concentration gradient does not affect the surface energy. We have neglected terms quadratic in the strain, which relate to the excess in the elastic stiffness of the epilayer relative to the substrate.

When the concentration field is uniform in the epilayer, the substrate is unstrained and $g(x_\alpha;C)$ is the only remaining term in eq 1. Hence $g(x_\alpha;C)$ represents the surface energy per unit area of a uniform epilayer on an unstrained substrate. To describe phase separation, we may prescribe $g(x_\alpha;C)$ as any function with double wells. In numerical simulations, to be definite, we assume that the epilayer is a regular solution and the function takes the form

$$g(x_\alpha;C) = g_A(x_1,x_2)(1-C) + g_B(x_1,x_2)C + \Lambda k_b T[C\ln C + (1-C)\ln(1-C) + \Omega C(1-C)] \qquad (2)$$

where $g_A(x_1,x_2)$ and $g_B(x_1,x_2)$ are the chemical potentials of pure components A and B attached to the substrate at position (x_1,x_2). For a homogeneous substrate surface, g_A and g_B become two constants. The first two terms in the bracket result from the entropy of mixing, and the third term from the enthalpy of mixing. Λ is the number of atoms per unit area on the surface, k_b is Boltzmann's constant, and T is the absolute temperature. The dimensionless number Ω measures the bond strength relative to the thermal energy k_bT. When $\Omega < 2$, the function g is convex. When $\Omega > 2$, the function g has double wells and drives phase separation. We assume that $h = h_0$ is a positive constant. Any nonuniformity in the concentration field by itself increases Γ. In the phase field model, the h-term in eq 1 represents the phase boundary energy. It drives phase coarsening. The quantity, f, known as surface stress, is the surface energy change associated with the elastic strain. As discussed, the concentration-dependent surface stress drives phase refining. We assume that surface stress is a linear function of the concentration, i.e., $f = \psi + \phi C$, where ψ and ϕ are material constants.[9] It should be noted that surface chemistry may also affect surface stress f and the coefficient h. This paper focuses on its effect through the free energy g. We have assumed that f and h do not explicitly depend on the coordinates.

The diffusion equation is given by[12−14]

$$\frac{\partial C}{\partial t} = \frac{M}{\Lambda^2}\nabla^2\left(\frac{\partial g}{\partial C} - 2h_0\nabla^2 C - \frac{(1-\nu^2)\phi^2}{\pi E}\int\int\frac{(x_1-\xi_1)\dfrac{\partial C}{\partial \xi_1} + (x_2-\xi_2)\dfrac{\partial C}{\partial \xi_2}}{[(x_1-\xi_1)^2 + (x_2-\xi_2)^2]^{3/2}}\,d\xi_1\,d\xi_2\right) \qquad (3)$$

where $\nabla^2 = \partial^2/\partial x_1^2 + \partial^2/\partial x_2^2$ and M is the mobility of atoms in the epilayer. The integration extends over the substrate surface. The strain field expressed by the double integration term is obtained by the superposition of the point force solution. Now consider the first two terms in eq 2, which depend on the coordinates explicitly. It should be noted that $g_A(x_1,x_2)$ by itself does not influence diffusion. This can be observed from eq 3, which relates to the function g only in terms of $\partial g/\partial C$. The effective part is $(g_B(x_1,x_2) - g_A(x_1,x_2))C$. In other words, only the chemical potential difference of the two components matters. This can also be understood from

another point of view. The contribution of $g_A(x_1,x_2)$ to the free energy, $\int\int g_A(x_1,x_2)\,dS$, is fixed and independent of any concentration change. Consequently, it does not influence diffusion. A dimensionless function $\mu_{B-A}(x_1,x_2)$ is defined by $\mu_{B-A}(x_1,x_2) = (g_B - g_A)/\Lambda k_b T$.

A comparison of the first two terms in the parentheses of eq 3 defines a length $b = \sqrt{h_0/\Lambda k_b T}$. In the Cahn-Hilliard model this length scales the phase boundary thickness. The magnitude of h_0 is on the order of energy per atom at a phase boundary. Using magnitudes $h_0 \sim 10^{-19}$ J, $\Lambda \sim 5 \times 10^{19}$ m^{-2}, and $k_b T \sim 5 \times 10^{-21}$ J (corresponding to $T = 400$ K), we have $b \sim 0.6$ nm. Another length, $l = Eh_0/[\phi^2(1-\nu^2)]$, is defined by comparing the last two terms in the parenthesis. This length reflects the competition of surface stress and phase boundary. Young's modulus of a bulk solid is about $E \sim 10^{11}$N/m^2. A representative value for ϕ is ~4N/m.[9] The equilibrium phase size is on the order $\sim 4\pi l$, according to theoretical analysis and simulation.[6,14] These magnitudes, together with $h_0 \sim 10^{-19}$ J, give $4\pi l \sim 8$ nm, broadly agrees with observed phase sizes in experiments. From eq 3, disregarding a dimensionless factor, we note that the diffusivity scales as $D \sim Mk_bT/\Lambda$. To resolve events occurring over the length scale of b, the time scale is $\tau = b^2/D$, namely $\tau = h_0/[M(k_bT)^2]$.

The integral makes it inefficient to solve eq 3 in real space. An efficient method is to solve the equation in reciprocal space. The Fourier transform converts the integral-differential equation into a regular partial differential equation. The integration operation, as well as the differentiation over space, is removed and the evolution equation is dramatically simplified. Let k_1 and k_2 be the coordinates in reciprocal space. Denote the Fourier transform of $C(x_1,x_2,t)$ by $\hat{C}(k_1,k_2,t)$, namely, $\hat{C}(k_1,k_2,t) = \int_{-\infty}^{\infty}\int_{-\infty}^{\infty} C(x_1,x_2,t)e^{-i(k_1x_1+k_2x_2)}\,dx_1\,dx_2$. Normalizing eq 3 by the length b and the time τ, and applying the Fourier transform on both sides, we obtain the evolution equation in reciprocal space

$$\frac{\partial \hat{C}}{\partial t} = k^2\hat{P} - 2(k^4 - k^3Q)\hat{C} \qquad (4)$$

where $k = \sqrt{k_1^2+k_2^2}$, $Q = b/l$, and $\hat{P}(k_1,k_2,t)$ is the Fourier transform of $P(x_1,x_2,t) = \mu_{B-A} + \ln(C/(1-C)) + \Omega(1-2C)$.

Selected simulation results are shown in Figures 2−4. The calculation cell size is $256b \times 256b$. Material parameters are $\Omega = 2.2$, $\nu = 0.3$, $Q = 1$. At a given time, the concentration fields are visualized by grayscale graphs. The darker region corresponds to higher concentration and the brighter region corresponds to lower concentration. The calculations start from random initial conditions. The boundary condition conditions are periodic. Figure 2 shows an evolution sequence guided by surface chemistry. The distribution of μ_{B-A} is given in Figure 2a, where the value is 0.1 in the six blue lines and 0 in other regions. The concentration has an average of 0.4. The initial concentration fluctuates randomly within 0.001 from the average. An epilayer would evolve into a pattern shown in Figure 3a when μ_{B-A} is uniform. The inhomogeneous surface chemistry

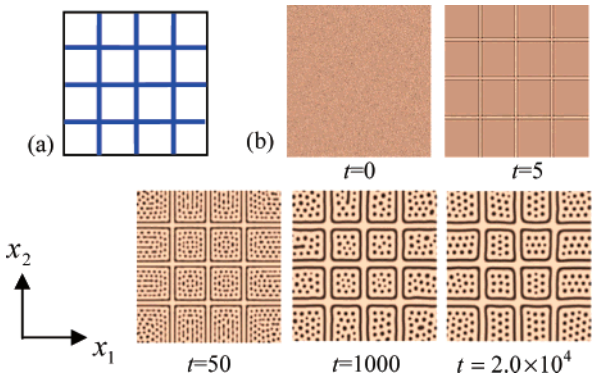

Figure 2. An evolution sequence guided by surface chemistry. (a) The distribution of μ_{B-A}; $\mu_{B-A} = 0.1$ in the six blue lines and $\mu_{B-A} = 0$ in other regions. (b) An evolution sequence from a random initial condition. The average concentration is 0.4.

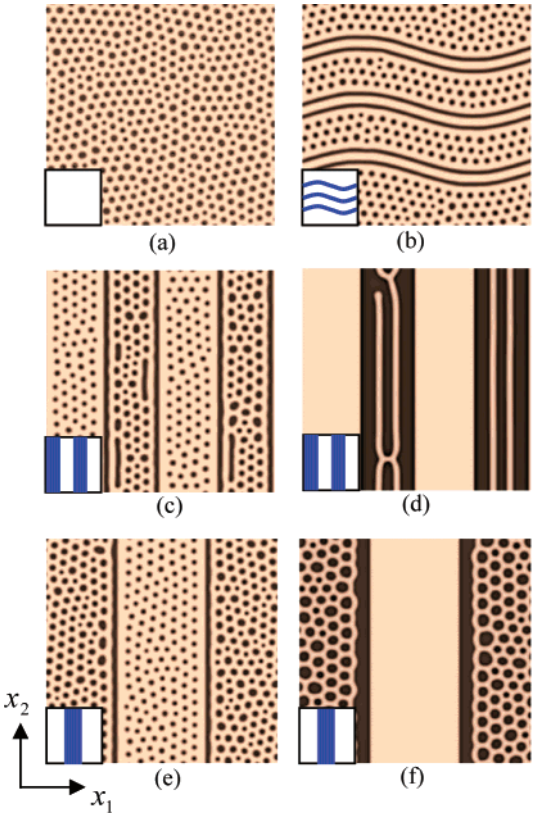

Figure 3. Various patterns at $t = 2.0 \times 10^4$ with average concentration 0.4. The small picture at the left bottom corner of each graph illustrates the distribution of μ_{B-A}. The white region has $\mu_{B-A} = 0$. In the blue regions, μ_{B-A} is 0.1 for (b), 0.05 for (c),(e), and 0.5 for (d),(f).

induces the accumulation of A-atom in the blue region and B-atom in the white region. An ordered lattice of dots forms in each small cell defined by the prepatterns of μ_{B-A}. Figure 3 shows various patterns at $t = 2.0 \times 10^4$ with average concentration 0.4. The small picture at the left bottom corner of each graph illustrates the distribution of μ_{B-A}. The white region has $\mu_{B-A} = 0$. A uniform μ_{B-A} leads to a triangular lattice of dots shown in Figure 3a. Figure 3b shows the pattern under the guidance of three sinusoidal curves. The blue curves have $\mu_{B-A} = 0.1$. The dots still form a triangular lattice, but orientate along the curves. The expelled B-atoms

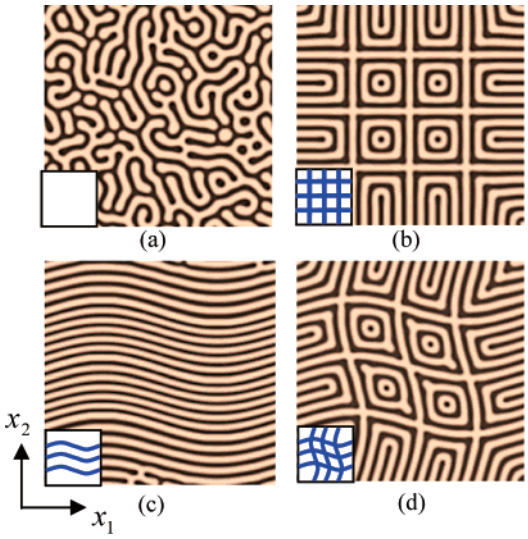

Figure 4. Various patterns at $t = 2.0 \times 10^4$ with average concentration 0.5. The small picture at the left bottom corner of each graph illustrates the distribution of μ_{B-A}. The white region has $\mu_{B-A} = 0$ and the blue region has $\mu_{B-A} = 0.1$.

accumulate around the bright A-rich sinusoidal curves, forming a dark boundary layer to separate the sinusoidal curves and dots.

The degree of nonuniformity in μ_{B-A} can be significant. Figures 3c and d show the patterns guided by alternating blue and white stripes. In Figure 3c the blue stripes have $\mu_{B-A} = 0.05$. The accumulation of B atoms in the white region increases the local average concentration, leading to large-sized dots comparing to those in the blue region. In Figure 3d, the large μ_{B-A} ($= 0.5$) in the blue region induces a strong attraction of A-atoms and expilation of B-atoms. The effect is so strong that stripes appear instead of dots. Figures 3e,f demonstrate the similar effect, where the area of the blue region is half of the white region. Figure 4 shows various patterns with average concentration 0.5. A uniform μ_{B-A} leads to the pattern shown in Figure 4a. Figures 4b−d demonstrate diverse patterns obtained by surface chemistry.

In summary, the self-assembly of a binary epilayer on the substrate forms various concentration patterns by competition of phase separation, phase coarsening, and phase refining. When the substrate surface is homogeneous, highly symmetric patterns appear including triangular lattice of dots and serpentine stripes. The simulations reveal that surface chemistry can significantly influence the pattern formation process. It breaks the symmetry of the system and leads to various patterns. In addition, it anchors self-assembled features at specific locations.

Acknowledgment. This work was partially supported by the Faculty Research Grant from the University of Michigan.

References

(1) Kern, K.; Niebus, H.; Schatz, A.; Zeppenfeld, P.; George, J.; Comsa, G. *Phys. Rev. Lett.* **1991**, *67*, 855.
(2) Plass, R.; Last, J. A.; Bartelt, N. C.; Kellogg, G. L. *Nature* **2001**, *412*, 875.
(3) Pohl, K.; Bartelt, M. C.; de la Figuera, J.; Bartelt, N. C.; Hrbek, J.; Hwang, R. Q. *Nature* **1999**, *397*, 238.
(4) Umezawa, K.; Nakanishi, S.; Yoshimura, M.; Ojima, K.; Ueda, K.; Gibson, W. M. *Phys. Rev. B* **2001**, *63*, 35 402.
(5) Alerhand, O. L.; Vanderbilt, D.; Meade, R. D.; Joannopoulos, J. D. *Phys. Rev. Lett.* **1988**, *61*, 1973.
(6) Lu, W.; Suo, Z. *Metallkd.* **1999**, *90*, 956.
(7) Cammarata, R. C. *Prog. Surf. Sci.* **1994**, *46*, 1.
(8) Cammarata, R. C.; Sieradzki, K. *Annu. Rev. Mater. Sci.* **1994**, *24*, 215.
(9) Ibach, H. *Surf. Sci. Rep.* **1997**, *29*, 193.
(10) Ng, K.-O.; Vanderbilt, D. *Phys. Rev. B* **1995**, *52*, 2177.
(11) Suo, Z.; Lu, W. *J. Mech. Phys. Solids* **2000**, *48*, 211.
(12) Lu, W.; Suo, Z. *Phys. Rev. B* **2002**, *65*, 085401.
(13) Lu, W.; Suo, Z. *Phys. Rev. B* **2002**, *65*, 205418.
(14) Lu, W.; Suo, Z. *J. Mech. Phys. Solids* **2001**, *49*, 1937.
(15) Suo, Z.; Lu, W. *J. Nanopart. Res.* **2000**, *2*, 333.
(16) Cahn, J. W.; Hilliard, J. E. *J. Chem. Phys.* **1958**, *28*, 258.

NL035072D